FORMULÁRIO DE ENCAMINHAMENTO - PERIÓDICO

Imprimir

Nº PEDIDO PE000396996/2008

IDENTIFICAÇÃO DO PEDIDO

TÍTULO DO PERIÓDICO: JOURNAL OF PHARMACEUTICAL SCIENCES

ANO: 1993 VOLUME: 82 FASCÍCULO/MÊS: 2 SUPLEMENTO: ISSN:

AUTOR DO ARTIGO: MARIA TERESA LAMY-FREUND

TÍTULO DO ARTIGO: EFFECT OF AGGREGATION ON THE KINETICS OF AUTOXIDATION...

PÁGINA INICIAL: 162 PÁGINA FINAL: 166 TOTAL DE PÁGINAS: 5 BÔNUS UTILIZADOS: 0

FORMA DE ENVIO: E-MAIL

SITUAÇÃO DO PEDIDO: [ ] Atendido [ ] Repassado [ ] Cancelado

FORMA DO DOC.ORIGINAL: TOTAL DE PÁG.CONFIRMAÇÃO:

MOTIVO:

OBSERVAÇÃO: P/ SILVANA

FORMULÁRIO DE ENCAMINHAMENTO - PERIÓDICO

BIBLIOTECA-BASE

NOME: USP/CQ/DBD - DIVISÃO DE BIBLIOTECA E DOCUMENTAÇÃO

ENDEREÇO: AVENIDA PROFESSOR LINEU PRESTES, 950

CEP: 05508900 CIDADE-UF: SAO PAULO-SP

Nº PEDIDO PE000396996/2008

USUARIO: CPF: 32555652949

NOME: LYDIA BAYER BARBOSA

TEL: (11) 30916923 E-MAIL: comut@sbi.if.usp.br

SOLICITANTE: CÓDIGO ou CPF: 000344-1

NOME: USP/IF/SBI - SERVIÇO DE BIBLIOTECA E INFORMAÇÃO

TEL: (11) 30916923 E-MAIL: comut@sbi.if.usp.br

IDENTIFICAÇÃO DO PEDIDO

TÍTULO DO PERIÓDICO: JOURNAL OF PHARMACEUTICAL SCIENCES

ANO: 1993 VOLUME: 82 FASCÍCULO/MÊS: 2 SUPLEMENTO: ISSN:

AUTOR DO ARTIGO: MARIA TERESA LAMY-FREUND

TÍTULO DO ARTIGO: EFFECT OF AGGREGATION ON THE KINETICS OF AUTOXIDATION...

PÁGINA INICIAL: 162 PÁGINA FINAL: 166 TOTAL DE PÁGINAS: 5 BÔNUS UTILIZADOS: 0

FORMA DE ENVIO: E-MAIL

FORMA DO DOC.ORIGINAL: TOTAL DE PÁG.CONFIRMAÇÃO:

DESTINATÁRIO

NOME: USP/IF/SBI - SERVIÇO DE BIBLIOTECA E INFORMAÇÃO

ENDEREÇO: RUA DO MATÃO, TRAV. R, 187

CEP: 05508900 **CIDADE-UF:** SAO PAULO-SP

TEL: **E-MAIL** comut@sbi.if.usp.br

Recebi o pedido Nº Data _____/_____/_____ Assinatura_____

Voltar

Effect of Aggregation on the Kinetics of Autoxidation of the Polyene Antibiotic Amphotericin B

M. TERESA LAMY-FREUND*, VERGÍNIA F. N. FERREIRA‡, ADELAIDE FALJONI-ALÁRIO‡, AND SHIRLEY SCHREIER‡x

Received October 3, 1991, from the *Institute of Physics, University of São Paulo, C.P. 20516, CEP 01498, S. Paulo, Brazil, and the ‡Department of Biochemistry, Institute of Chemistry, University of São Paulo, C.P. 20780, CEP 01498, S. Paulo, Brazil. Accepted for publication June 8, 1992.

Abstract □ We have previously studied the autoxidation of the polyene antibiotic amphotericin B (AB). In this paper we describe the dependence of the kinetics of autoxidation on the aggregation state of the antibiotic. Autoxidation, which is involved in drug inactivation and has been suggested to play a role in the mechanism of drug action, was assessed through the reaction of formed radicals with the spin label Tempol (2,2,6,6-tetramethyl-4-hydroxy-*N*-oxylpiperidine) by following the loss of the electron spin resonance signal, as previously described, and by oxygen consumption. Two types of AB (I and II) were used, the former being obtained by further purification of the latter. The kinetics of autoxidation were compared for aggregates formed by the antibiotic. Differences in aggregation state for both type I and type II AB were observed between monomeric, borax-complexed, and preparations in water containing variable proportions of dimethyl sulfoxide (DMSO) by optical absorption and circular dichroism (CD) spectra. On the other hand, although the suspensions of type I and type II AB in water–10% DMSO did not differ in their optical properties, they could be distinguished by quasielastic light scattering experiments, type II yielding smaller aggregates. It is proposed that the lack of difference in optical and CD spectra are due to the similarity of the microenvironments in both aggregates. In contrast, the borax complex of both type I and type II AB yielded similar optical and CD spectra and quasielastic light scattering behavior, indicating that complexation led to similar aggregates. Whereas monomeric type I and type II AB displayed similar autoxidation kinetics, the aggregates formed in water–10% DMSO reacted at different rates, with type II yielding slower kinetics. Transition metal ion chelating agents had little, but equivalent, or no effects on the kinetics of autoxidation. The borax complexes of type I and type II AB displayed similar kinetics. Oxygen consumption measurements were in agreement with the electron spin resonance results. Aggregation properties could be related to the mechanism of action and/or toxicity of the antibiotic.

Amphotericin B (AB) is primarily used in the treatment of systemic mycotic infections, despite its being extremely toxic, causing massive intravascular hemolysis and nephrotoxicity. It acts at the membrane level, altering membrane permeability by a mechanism thought to involve pore formation.[1] As a result of the presence of a hydrophobic region in the molecule, consisting of seven conjugated double bonds, and of its zwitterionic character, AB is very poorly soluble in aqueous media at physiological pH. In vivo studies with AB and other polyene antibiotics suggest that both therapeutic and toxic properties of these drugs might depend on aggregation.[2,3] Because many studies of the effects of AB on membranes are done with the aggregated antibiotic, Aracava et al.[4] suggested that aggregation may play a role in the mechanism of action of AB. On the other hand, the inactivation of the antibiotic has been proposed to involve autoxidation. Beggs and coworkers[5,6] have shown that antioxidants delay AB inactivation. Rickards et al.[7] established the chemical nature of the major products of the autoxidation of filipin and lagosin, but were unable to detect free radicals by electron spin resonance (ESR), possibly because of their low steady-state concentration. Autoxidation of AB and other polyene antibiotics in dimethyl sulfoxide (DMSO) was examined by Gutteridge et al.[8] through the reaction between formed products and thiobarbituric acid. Free radicals were measured by ESR and have been suggested to be involved in the mechanism of inactivation of polyene antibiotics by Bronov et al.[9] Autoxidation of AB has also been suggested to mediate lipid peroxidation, thereby leading to the lytic effects of AB.[10]

We have previously demonstrated free radical formation during AB autoxidation.[11] Here we show that the kinetics of AB autoxidation are affected by its aggregation state.

Experimental Section

AB was provided by Squibb Indústria Química S.A., São Paulo, Brazil, and was stored at −10 °C in the dark. Two forms of crystalline AB were used: type II (~800 μg/mg) and type I (~900 μg/mg), which comes from the last stage of AB purification. Fungizone, which consists of AB:deoxycholate (1:2, mol:mol), was also a gift of Squibb Indústria Química S.A. Tempol (2,2,6,6-tetramethyl-4-hydroxy-*N*-oxylpiperidine) was a gift of Dr. Rolf Mehlhorn from the Department of Physiology and Anatomy, University of California, Berkeley, CA. DMSO was from Merck-Quimitra (Rio de Janeiro, Brazil), desferrioxamine was from Ciba Pharmaceutical Company (Basel, Switzerland), borax (sodium tetraborate) was from Carlo Erba (São Paulo, Brazil), and diethylenetriamine pentaacetic acid (DTPA) was from Sigma Chemical Company (St. Louis, MO). All reagents were analytical grade. Double-distilled deionized water was used throughout.

AB solutions were prepared immediately before use. AB was first dissolved in DMSO and then buffer was added. The samples were shaken for 1 min in a vortex mixer. The samples containing borax were prepared in a similar way, except that the buffer contained borax at either 100 mM [optical and circular dichroism (CD) spectra and ESR] or 1 mM [quasielastic light scattering (QELS)]. An NaCl–10 mM phosphate buffer (pH 7.4, 260 mOsm) was used throughout, except for the filtration and QELS experiments when pure double-distilled, deionized water was used because the high ionic strength greatly increases both aggregate size and polydispersity. AB concentrations were determined spectrophotometrically.

For filtrations, membranes of different pore size (Millipore, Burlington, MA) were used. ESR spectra were obtained with a Varian E-4 X-band spectrometer at room temperature (22 ± 2 °C). Flat quartz cells for aqueous solutions came from James Scanlon, Costa Mesa, CA. Oxygen consumption was measured in an oxygen biological monitor (model 53, Yellow Springs Instruments, Yellow Springs, OH). Oxygen consumption in pure DMSO solutions was determined by making use of the quenching effect of O_2 on the fluorescence of the ruthenium (II)–*tris*(bipyridyl) complex.[12] Optical absorption spectra were obtained with a DMR 10 Zeiss spectrophotometer. The CD spectra were obtained with a Cary (Varian, Palo Alto, CA) model 60 recorder spectropolarimeter equipped with a model 6002 accessory.

Dynamic light scattering experiments were made at room temperature (22 ± 2 °C) with a helium–neon laser (Hughes Aircraft Co., Carlsbad, CA) operated at 633 nm as the light source, and a BI 2030 instrument (Brookhaven Instruments Co., Ronkonkoma, NY) for autocorrelation of the scattered intensity signal.

Autocorrelation curves were taken consecutively at a fixed obser-

0022-3549/93/0200-0162$02.50/0

vation angle of 90°. Typically, there were 100 separate autocorrelation curves per run. A standard second-order cumulant analysis[13] was used for determining the z-average diffusion coefficient (D). The polydispersity index (Q) was calculated by eq 1:

$$Q = \frac{\mu_2}{\Gamma^2} \quad (1)$$

In eq 1, Γ and μ_2 are, respectively, the first and second moments of the expansion of the logarithm of the electric field autocorrelation function. Although the polydispersity values found are relatively high (Table I), the cumulants technique was used because the purpose of the QELS measurements was primarily an estimation of the difference in size distribution of the various aggregates under study.

For convenience and ease of interpretation, the equivalent hydrodynamic diameter (D_H), given by the familiar Stokes–Einstein equation (eq 2) was used, although it is quite possible that the aggregates studied are not spherical:

$$D_H = \frac{kT}{3\pi\eta D} \quad (2)$$

In eq 2, k is the Boltzmann constant, η is the viscosity, and D is the diffusion constant.

Results

Characterization of AB Aggregates—The AB aggregates were analyzed by optical and CD spectroscopy and by QELS. In DMSO, AB seems to be monomeric. The optical absorption spectrum is typical of the heptene chromophore, with a resolved vibronic structure.[14] Four principal bands are observed at 418, 388, 368, and 350 nm (Figure 1). AB remains monomeric when increasing proportions of buffer are added to DMSO solutions up to 40% buffer, aggregation taking place at higher proportions. In aqueous medium, above $\sim 10^{-4}$ M, AB is aggregated,[15,16] as indicated by a blue shift and concomitant disappearance of the vibronic structure (Figure 1). The asymmetry of the 340 nm band is suggestive of a polydisperse system. The intense CD spectrum of these aggregates (Figure 1) indicates an organized asymmetric structure. It should be noted that the spectra in Figure 1 correspond to samples containing 10% DMSO in volume. These results refer both to type I and type II AB.

The polydispersity of aggregated AB is also evinced by QELS (Table I) and by filtration (Table II) experiments. In spite of the inaccuracy involved in the latter experiment, the results (Table II) show that when samples of type I and type II AB are filtered through membranes of variable pore size, the particle size distribution is in reasonable agreement with that obtained by QELS (Table I).

Although aggregated AB in buffer–10% DMSO is polydisperse, a rough estimate of the degree of organization was performed by calculating the anisotropy of the system with the ratio $\theta°/A$, where $\theta°$ is the ellipticity, measured from the CD spectra, and A is the absorbance. The anisotropy of the aggregates is ~50 times higher than that of the monomer (Table III).

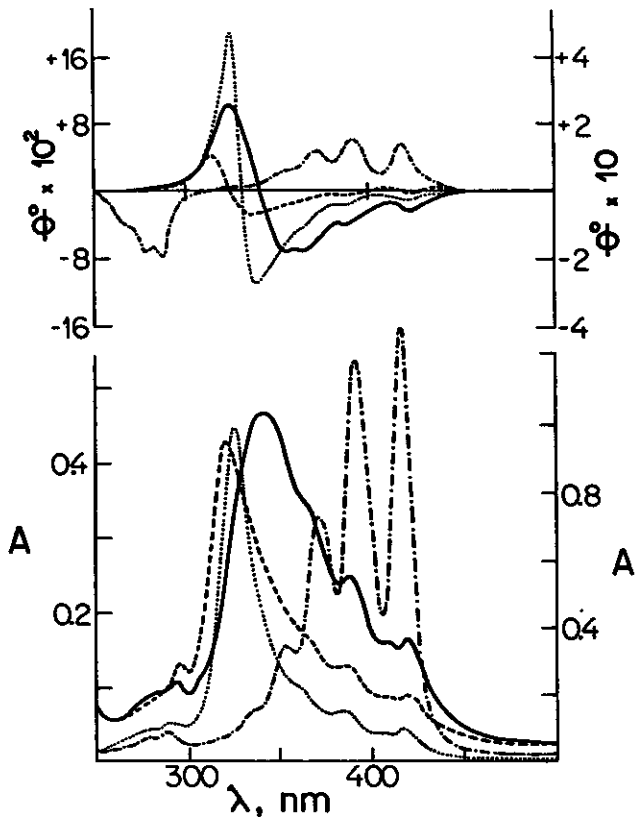

Figure 1—Optical absorption (bottom) and CD (top) spectra of 0.1 mM AB. Key: monomeric in DMSO (-.-.-.-); in buffer–10% DMSO (———); in buffer–10% DMSO–100 mM borax (- - - -); fungizone (. . .). See *Experimental Section* for details. Path length was 0.1 cm. The right-hand scale corresponds to monomeric AB (bottom) and to fungizone (top and bottom). The CD spectrum for monomeric AB is expanded by a factor of 10.

Table II—Percentage of AB Recovered after Filtration through Membranes of Different Pore Size[a,b]

Pore Size, μm	AB	
	Type I	Type II
1.20	75	84
0.80	55	75
0.45	21	50
0.22	4	16
0.10	2	3

[a] [AB] = 0.1 mM in water–10% DMSO. [b] The values are the mean average of three determinations, with a maximum deviation of 10%.

In spite of the similarity of the optical and CD spectra for type I and type II AB aggregates in buffer–10% DMSO, QELS measurements yield very different values for particle size and

Table I—QELS Determination of Equivalent Hydrodynamic Diameter (D_H), Polydispersity (Q), and Diffusion Coefficients (D) of Type I and Type II AB Aggregates and of Their Borax Complexes in Water–10% DMSO[a,b]

Medium	Aggregate Type	n[c]	D_H, μm	Q	$D \times 10^{-9}$, cm²/s
Water–10% DMSO	I	15	0.901 ± 0.121	0.369 ± 0.082	3.67 ± 0.73
	II	11	0.275 ± 0.026	0.333 ± 0.054	9.32 ± 2.43
+1 mM Borax	I	10	0.215 ± 0.028	0.431 ± 0.106	8.76 ± 4.83
	II	9	0.197 ± 0.014	0.433 ± 0.063	11.55 ± 3.34

[a] [AB] = 0.1 mM. [b] The values are mean ± standard error. [c] Number of experiments.

Table III—Anisotropy of AB Aggregates[a]

AB Preparation	$\theta° \times 10^3$	A	$\theta°/A \times 10^3$
In buffer–10% DMSO	+106 (325)	0.47 (340)	226
In buffer–10% DMSO + 100 mM borax	+ 43 (314)	0.43 (319)	100
Fungizone	+446 (324)	0.98 (327)	476
In pure DMSO	+ 5.6 (416)	1.28 (418)	4.4

[a] The numbers in parentheses are the wavelengths at which A and $\theta°$ were measured; [AB] = 0.1 mM; path length = 0.1 cm.

diffusion coefficients, indicating that the aggregates are different (Table I). These data are corroborated by the filtration results (Table II).

The solubility of AB increases on complexation with borax, as described by Strauss and Kral.[17] Our preparation was somewhat different from that of these authors (see *Experimental Section*). Clearly, complexation alters the structure of the aggregates (Figure 1), the 340 nm band being shifted to 319 nm. We found a factor of $\sim 5 \times 10^2$ difference in the value of ϵ (molar absorptivity) with respect to that reported by Strauss and Kral.[17] The optical spectra of the AB–borax complex coincide for type I and type II AB. In contrast with the uncomplexed aggregated antibiotic, in this case, QELS measurements yield similar values for particle size, polydispersity, and diffusion coefficients of the complexes (Table I), strongly suggesting that complexation leads to similar final structures. The anisotropy of the AB–borax aggregate is ~2.3 times smaller than that of aggregated AB in buffer–10% DMSO (Table III), suggesting a looser structure for the complex.

For comparison, we also present the optical spectra of fungizone, which corresponds to a more homogeneous system. The amplitude of the absorption band of fungizone is about twice that obtained for either AB or AB–borax aggregates, and the CD doublet is even relatively more intense, yielding a very high degree of anisotropy (Table III).

Kinetics of AB Autoxidation: Role of Aggregation—Autoxidation was monitored by following the reaction of the formed radicals with Tempol through the decay of its ESR signal and by measurement of oxygen consumption.[11] Previous studies with the spin trap phenyl-*t*-butyl nitrone (PBN) indicated formation of DMSO spin adducts.[11] Although aggregation probably depends on concentration, for technical reasons, optical spectra and QELS measurements were performed at 0.1 mM AB, whereas 5 mM AB was used for ESR studies.

Monomeric type I and type II AB display similar autoxidation rates (Figure 2). Analogous results were obtained for solvent systems containing 100, 99, and 90% DMSO. Under these conditions, AB is monomeric (see previous section). As aggregation occurs (~60% DMSO), type I and type II AB start to present different kinetics, the autoxidation rate being faster for the former. The differences between the two preparations in buffer–10% DMSO are illustrated in Figure 3. The times required for the decay of 30% of the ESR signal for Tempol are indicated in Table IV. The use of this parameter has been justified previously.[11] It should be noted that, when aggregated, type I and type II AB display different kinetics of autoxidation, regardless of the solvent system (buffer–DMSO or water–DMSO). Because type I and type II AB originate from different stages of antibiotic purification, the different kinetics could be due to impurities that might influence radical formation rather than to different aggregation.

To check for the possibility of spurious metal ion catalysis, two chelating agents were used, DTPA and desferrioxamine.[18,19] DTPA, which chelates transition metal ions nonspecifically,[20] had no effect on the kinetics of the Tempol signal loss. However, because the DTPA–iron complex also catalyses radical processes,[21] desferrioxamine, whose iron complex is considered not to act catalytically,[21] was also employed. Desferrioxamine inhibits the formation of radicals to a similar degree both for type I and for type II AB, but the Tempol

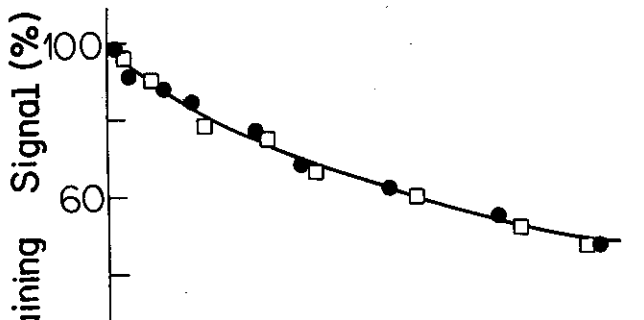

Figure 2—Kinetics of Tempol (5 μM) ESR signal decay for 5 mM type I (●) and type II (□) AB in DMSO.

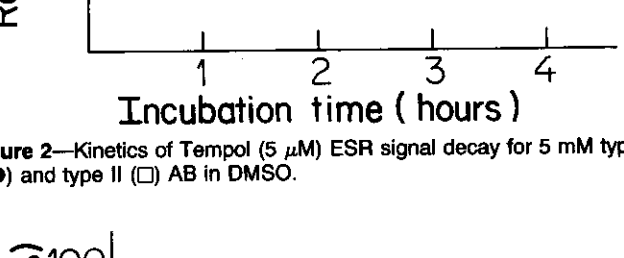

Figure 3—Kinetics of Tempol (5 μM) ESR signal decay for 5 mM AB in buffer–10% DMSO. Key: type I AB (●, ○) and type II AB (■, □) in the absence (closed symbols) and presence (open symbols) of 0.10 mM desferrioxamine.

Table IV—Time Required for Loss of 30% Tempol ESR Signal for Different AB Preparations[a]

Medium	Time (min) for: Type I AB	Type II AB
Buffer–10% DMSO	18 ± 2 (11)	38 ± 4 (11)
Buffer–10% DMSO + 100 mM borax	35 ± 5 (5)	38 ± 5 (5)
Buffer–10% DMSO + 0.1 mM desferrioxamine	26 ± 1 (2)	46 ± 1 (2)
Pure DMSO	95 ± 6 (5)	98 ± 4 (5)

[a] [AB] = 5 mM; [Tempol] = 5 μM; the values are mean ± standard error; the number of experiments is given in parentheses.

signal loss does not depend on the presence of metal ions (iron) to a large extent (Figure 3, Table IV). The difference between the two types of AB is maintained after the removal of the effect of metal ions.

Comparison of the kinetics of the Tempol ESR signal decay for type I AB in buffer–10% DMSO with those of its borax complex (Figure 4) indicates that the AB–borax complex reacts more slowly, suggesting a correlation between differences in aggregation as reported by optical and CD spectra and differences in the rate of radical formation. No difference was observed between the rates of autoxidation of type II AB and its borax complex (Table IV). Of all the cases examined in the present study, this is the only one in which a difference was observed in the aggregation state that was not accompanied by changes in the kinetics of autoxidation. Other than being a coincidence, we have no explanation at present for this result. It is worthwhile to notice that both type I and type II AB borax complexes display similar autoxidation rates, in agreement with the QELS data (Table I), suggesting that both types give rise to similar aggregates on complexation.

The effect of borax does not seem to be due to a nonspecific increase of ionic strength because 0.3 M NaCl neither changes the AB optical spectra nor alters the kinetics of Tempol signal decay.

In agreement with the ESR results, measurements of oxygen consumption show that in buffer–10% DMSO, type I AB reacts faster than type II, whereas in DMSO, both types display similar rates of oxygen consumption (Table V).

Discussion

Several interrelated factors, such as oxygen concentration, metal ion content, reaction medium, and aggregation state, could affect the rate of AB autoxidation. Evidence for the role of aggregation in this process is provided in this study. The results of the experiments described clearly indicate that differences in the kinetics of AB autoxidation are observed between monomeric and aggregated AB. Although it is reasonable to expect medium effects on reaction kinetics, the results show that for the same medium the rates of radical formation are invariant for monomeric AB (type I and type II) but are significantly affected for aggregated AB.

The kinetics of Tempol signal decay are similar for monomeric type I and type II AB in DMSO (Figure 2, Table IV) and in buffer–DMSO mixtures containing enough of the latter

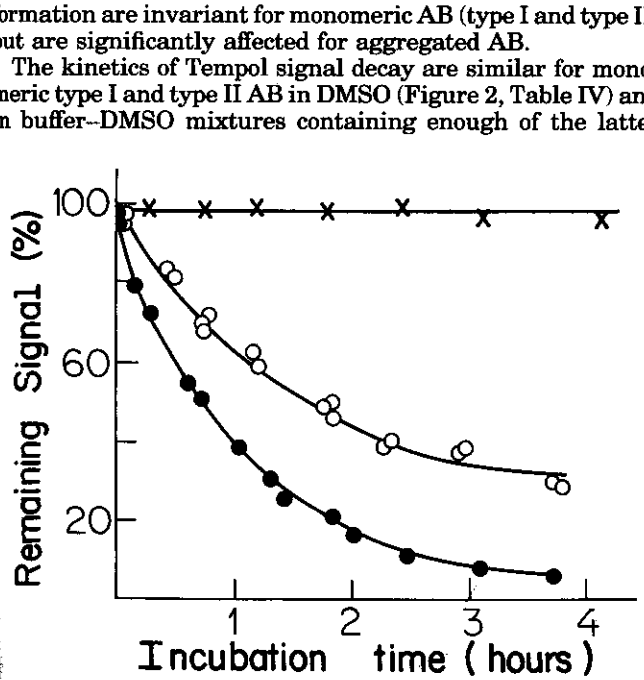

Figure 4—Kinetics of the ESR signal decay of 5 μM Tempol in the presence of 5 mM type I AB in buffer–10% DMSO (●) and in buffer–10% DMSO–100 mM borax (○). Control (X) was 5 μM Tempol in buffer–10% DMSO (see *Experimental Section* for details).

Table V—Time Required for 30% Oxygen Consumption for Different AB Preparations[a]

Medium	Time (min) for:	
	Type I AB	Type II AB
Buffer–10% DMSO	40, 48	100, 120
Pure DMSO	92	90

[a] [AB] = 5 mM.

solvent to keep the antibiotic monomeric. In contrast, in buffer–10% DMSO, different rates of signal loss (Figure 3, Table IV) and of oxygen consumption (Table V) are observed.

Although optical and CD spectra (Figure 1) do not reveal differences between type I and type II AB in buffer–10% DMSO, QELS (Table I) and filtration (Table II) data indicate that their aggregates differ in size and diffusion coefficient. Optical and CD spectra of AB arise from the interaction between few molecules of the aggregated species.[15,16] Thus, types I and II AB seem to form aggregates with different sizes but with similar microenvironments.

The metal complexing studies indicate that the differences between types I and II AB are not due to metal ion content (Figure 3). Moreover, type I AB, which originates from the last stage of antibiotic purification, autoxidizes faster than type II AB.

The optical spectra of AB change on addition of borax (Figure 1). Because borax interacts with –OH and possibly $-NH_2$ groups,[17] intercalation of borate between stacked antibiotic molecules could give rise to a looser structure. Although a large degree of inaccuracy could be involved in estimating the anisotropy of polydisperse AB, the smaller anisotropy of borax-complexed AB (Table III) is suggestive of a looser structure.

In agreement with the structural changes revealed by optical and CD spectroscopy, the AB (type I)–borax complex yields different (slower) kinetics of autoxidation (Figure 4, Table IV). The lack of change in the autoxidation kinetics of the borax complex of type II AB when compared with the antibiotic in buffer–10% DMSO (Table IV) could be a coincidence. The similarity of particle properties for the borax complexes of types I and II AB, as revealed by QELS (Table I), is indicative of similar complexes being formed on complexation and correlates well with the similar autoxidation rates displayed by both types of AB (Table IV).

The present results indicate that aggregation plays a role in the chemical reactivity of the antibiotic. Aggregation has also been found to affect the kinetics of lipid peroxidation processes.[22]

Chemical reactivity has been implied in the inactivation[5,6] and mechanism of action[10] of AB. The mechanism of action and toxicity of AB might also be affected by its state of organization. Several studies have indicated a correlation between particle size and structure and therapeutic and toxic effects of AB and other polyene antibiotics.[2,3] Lamy-Freund et al.[23,24] have shown that the size, composition, and solubility of AB–deoxycholate (fungizone) mixed aggregates depend on concentration. Bolard and co-workers[25] have shown that whereas monomeric AB interacts with ergosterol-containing liposomes, cholesterol-containing membranes bind the aggregated antibiotic. Thus, in studies with AB, it is important to take into account the organizational state of the antibiotic.

References and Notes

1. Medoff, G.; Kobayashi, G. S. *Ann. Rev. Pharmacol. Toxicol.* **1983**, *23*, 303–330.
2. Bennett, J. E.; Hill, G. J., II; Buttler, W. T.; Emmons, C. W. *Antimicrob. Agents Chemother.* **1964**, 745–752.

3. Ghielmetti, S.; Bruzzese, T.; Bianchi, C.; Recusani, F. *J. Pharm. Sci.* **1976**, *65*, 905–907.
4. Aracava, Y.; Smith, I. C. P.; Schreier, S. *Biochemistry* **1981**, *20*, 5702–5707.
5. Andrews, F. A.; Beggs, W. H.; Sarosi, G. A. *Antimicrob. Agents Chemother.* **1977**, *11*, 615–618.
6. Andrews, F. A.; Sarosi, G. A.; Beggs, W. H. *J. Antimicrob. Chemother.* **1979**, *5*, 173–177.
7. Rickards, R. W.; Smith, R. M.; Golding, B. T. *J. Antibiot.* **1970**, *23*, 603–612.
8. Gutteridge, J. M. C.; Thomas, A. M.; Cuthbert, A. *J. Appl. Biochem.* **1983**, *5*, 53–58.
9. Bronov, L. V.; Kolosova, O. M.; Kroshilova, T. M.; Ivanov, G. C.; Krunchak, V. G.; Komarov, E. V.; Fradkova, T. A. *Antibiotiki* **1982**, *22*, 585–588.
10. Brajtburg, J.; Elberg, S.; Schwartz, D. R.; Vertut-Croquin, A.; Schlessinger, D.; Kobayashi, G. S.; Medoff, G. *Antimicrob. Agents Chemother.* **1985**, *27*, 172–176.
11. Lamy-Freund, M. T.; Ferreira, V. F. N.; Schreier, S. *J. Antibiot.* **1985**, *38*, 753–757.
12. Sasso, M. G.; Quina, F. H.; Bechara, E. J. H. *Anal. Biochem.* **1986**, *156*, 239–243.
13. Koppel, D. E. *J. Chem. Phys.* **1972**, *57*, 4814–4820.
14. Hammond, S. M. *Prog. Med. Chem.* **1977**, *14*, 105–179.
15. Ernst, C.; Grange, J.; Rinnert, H.; Dupont, G.; Lematre, J. *Biopolymers* **1981**, *20*, 1575–1588.
16. Mazerski, J.; Bolard, J.; Borowski, E. *Biochim. Biophys. Acta* **1982**, *179*, 11–17.
17. Strauss, G.; Kral, F. *Biopolymers* **1982**, *21*, 459–470.
18. Gutteridge, J. M. C.; Richmond, R.; Halliwell, B. *Biochem. J.* **1979**, *184*, 469–472.
19. Graf, E.; Mahoney, J. R.; Bryant, R. G.; Eaton, J. W. *J. Biol. Chem.* **1984**, *259*, 3620–3624.
20. Chaberek, S.; Frost, A. E.; Doran, M. A.; Bicknell, N. J. *J. Inorg. Nucl. Chem.* **1959**, *11*, 184–196.
21. Geep, P.; Davison, A. J. *Biochim. Biophys. Acta* **1985**, *838*, 183–190.
22. Barclay, L. R. C.; MacNeil, J. M.; Van Kessel, J. A.; Forrest, B. J.; Porter, N. A.; Lehman, L. S.; Smith, K. J.; Ellington, J. C., Jr. *J. Am. Chem. Soc.* **1984**, *106*, 6740–6747.
23. Lamy-Freund, M. T.; Ferreira, V. F. N.; Schreier, S. *Biochim. Biophys. Acta* **1989**, *981*, 207–212.
24. Lamy-Freund, M. T.; Schreier, S.; Peitzsch, R.; Reed, W. F. *J. Pharm. Sci.* **1991**, *80*, 262–266.
25. Bolard, J.; Legrand, P.; Heitz, F.; Cybulska, B. *Biochemistry* **1991**, *30*, 5707–5715.

Acknowledgments

We thank Ms. Alice H. Ichikawa and Mr. Maurício S. Baptista for doing the QELS measurements. We are grateful to Dr. Marisa H. G. Medeiros for valuable suggestions and to Dr. Ohara Augusto for helpful discussions. This work was supported by Fundação de Amparo à Pesquisa do Estado de São Paulo (FAPESP), Conselho Nacional de Desenvolvimento Científico e Tecnológico (CNPq), and Financiadora de Estudos e Projetos (FINEP). M.T.L.F., A.F.A., and S.S. are recipients of research fellowships from CNPq. V.F.N.F. was the recipient of an undergraduate scholarship from FAPESP. We thank Miss Elisety de Andrade Silva for typing the manuscript.